

Fabric-Elasticity Relationships of Tibial Trabecular Bone are Similar in Osteogenesis Imperfecta (OI) and Healthy Individuals

Mathieu Simon^a, Michael Indermaur^a, Denis Schenk^a, Bettina Willie^{b,c}, Mahdi T.^{b,c}, Bettina M. Willie^{b,c} and Philippe Zysset^a

^aARTORG Centre for Biomedical Engineering Research, University of Bern, Bern, Switzerland

^bResearch Centre, Shriners Hospital for Children, Montreal, Canada

^cDepartement of Pediatric Surgery, McGill University, Montreal, Canada

ARTICLE INFO

Keywords:

Bone
Elasticity
Fabric
Osteogenesis Imperfecta

ABSTRACT

Osteogenesis Imperfecta (OI) is an inherited form of bone fragility. This disease, also called "brittle bone disease". It is characterised by impaired synthesis of type I collagen, altered trabecular bone architecture and reduced bone mass that lead to fragile bones. High resolution peripheral computed tomography (HR-pQCT) is a powerful method to investigate bone morphology in extremities including the weight-bearing distal tibia and the . The resulting 3D reconstructions can be exploited in either used as a basis of micro-finite element (μ FE) or homogenised finite element (hFE) analysis models for bone strength estimation. The hFE scheme uses homogenized local bone volume fraction (BV/TV) and anisotropy information (fabric) to compute healthy bone strength within a reasonable computation time using fabric-elasticity relationships. Thus, the aim of this study is to investigate fabric-elasticity relationships in OI trabecular bone compared to healthy controls.

In this study, the morphology of distal tibias of tibiae from 50 OI diagnosed people adults with OI were compared to 120 healthy controls using second generation HR-pQCT. Six cubic regions of interest (ROIs) were selected per individual in a common anatomical region. A first age & gender matching was performed by selecting similar individuals to obtain identical mean and median age and gender distribution in the OI and healthy control group. It allowed to perform a morphometric analysis and compare the outcome with literature. Then, stiffness tensors of ROIs were computed by FEA using hFEA and multiple linear regressions were performed on the Zysset-Curnier orthotropic model. The regressions allowed to compare the two groups using 5 parameters. After initial fits with all the samples of each group , the An initial fit was performed on both the OI group and the healthy control group using all the ROIs extracted. Then, data were filtered according to a fixed threshold for a defined coefficient of variation (CV) assessing the ROI heterogeneity . Second and second fits were performed on these filtered data sets and then additional fits were done on BV/TV & fabric anisotropy (DA) matched data to detect statistical differences between the two groups. These full and filtered data were in turn compared with previous results from μ CT reconstructions obtained in other anatomical locations. Finally, the ROIs of both group were matched according to their BV/TV and fabric anisotropy (DA). Fits were performed again using these matched data to detect statistical differences between the two groups.

In agreement with available literature, Compared to healthy controls, we found the OI samples to have significantly lower BV/TV and trabecular number (TbN.N.), significantly higher trabecular spacing (TbSp), separation (Tb.Sp.) and trabecular spacing standard deviation (TbSp.Sp.SD), but no differences in trabecular thickness (TbTh) were found between OI and controls.Th.). These results are in agreement to literature. The stiffness of ROIs from OI bone reached lower values compared to healthy controls and the multilinear fabric-elasticity fits tended to overestimate the stiffness in the lower range. Filtering out The filtering of highly heterogeneous ROIs removed these low stiffness ROIs and lead to similar correlation coefficients for both OI and healthy groups. Finally, the BV/TV & and DA matched data revealed no significant differences in fabric-elasticity parameters between OI and healthy individuals. Comparing with Compared to previous studies, the stiffness constants from the 61 μ m resolution HR-pQCT ROIs were lower than for the 36 μ m resolution μ CT images μ m resolution μ CT ROIs.

In conclusion, despite the reduced regression parameters found for HR-pQCT images, the fabric-elasticity relationships between OI and healthy individuals are similar when the trabecular bone ROIs are sufficiently homogeneous to perform the mechanical analysis. Since highly heterogeneous ROIs coincide with very low BV/TV, we expect them to play a minor role in hFE analysis of distal bone sections or parts.

Abbreviations: OI, osteogenesis imperfecta; HR-pQCT, high resolution peripheral quantitative computed tomography; BMD, bone mass density; ROI, region of interest; BV/TV, bone volume over total volume; SMI, structure model index; MIL, mean intercept length; FEA, finite element analysis KUBC, kinematic uniform boundary condition; PMUBC, periodicity-compatible mixed uniform boundary condition.

Email addresses: mathieu.simon@artorg.unibe.ch (M. Simon)

1. Introduction

Osteogenesis imperfecta (OI), also commonly known as "brittle bone disease", is an inherited form of bone fragility [25]. It was estimated to concern OI prevalence is estimated at about 1/13,500 of births, less severe forms being not accounted in this estimation as they are recognized later in life [15]. Therefore, OI is considered as a rare metabolic bone

disorder. Sillence classification [?] allows to define four main types of OI based on the clinical phenotype. In most cases, OI is caused by mutations in genes encoding type I collagen (COL1A1 and COL1A2), leading to brittle and fragile bones [14], as well as deformed geometry and size in some cases. OI can be categorized according to disease severity [18] into:

- Type I: less severe mild
- Type II: lethal at most shortly after birth perinatally lethal
- Type III: most severe surviving form
- Type IV: intermediate severity

Also known as "brittle bone disease", OI is characterized by impaired synthesis of type I collagen, leading to such brittle and fragile bones [14].

Bone fragility in OI is complex and not totally understood, despite the investigations at different hierarchical levels. Multiple studies show that DXA areal BMD (bone mineral density) (aBMD) tends to be lower in OI than compared to healthy individuals [7, 15, 24]. The microstructure is different as well. Folkestad et al.[7], Kocjan et al.[12], and Rolvien et al.[22] shown that have shown that the microstructure is different as well, namely bone volume fraction (BV/TV) and trabecular number in OI (Tb.N.) in OI bone is lower than for healthy controls. Trabecular spacing and inhomogeneity separation (Tb.Sp.) and inhomogeneity (Tb.Sp.SD) are higher for OI diagnosed people individuals with OI but the trabecular thickness (Tb.Th.) is not significantly different. At the ECM level, a recent study showed that, in compression, OI bone tends to present higher modulus, ultimate stress and post-yield behavior than healthy bone in compression, mostly affected by the higher degree of mineralization of OI bone [11].

High resolution peripheral quantitative computed tomography (HR-pQCT) scans allow one to perform *in vivo* assessment of cortical and trabecular architecture and volumetric BMD in bone mineral density (BMD) in the distal radius and distal tibia [3]. Moreover, the bony microstructure image obtained from HR-pQCT can be used for finite element analysis (FEA) to predict mechanical properties [4]. Homogenized FE finite element (hFE) is a FEA scheme including volume fraction (based on BV/TV) and anisotropy information (fabric) of trabecular bone from the HR-pQCT which scan that can be used to assess bone strength within a reasonable computation time [19]. High correlations were found between patient-specific hFE and mechanical compression experiment of cadaveric samples experiments of freshly frozen human samples at the distal radius [26, 2]. Thus, it could be legitimate to use hFE for OI patients patient's bone strength estimation and potentially fracture risk assessment. However, HR-pQCT-based FEA rely relies on fabric-elasticity relationships. Therefore, the present study aims to compare trabecular bone microstructure of healthy

and OI diagnosed individuals bone samples and to investigate the hypothesis of similar fabric-elasticity relationships.

2. Methods

2.1. Subjects Participants

The healthy group include included a total of 120 patients from a previous reproducibility study performed at the University Department of osteoporosis in Bern [23]. The sample is group was composed of 64 female females and 56 male subjects males aged between 20 and 92 years old with a median age of 26.22–35 mean age of 32 ± 15 years. These subjects did not took had not taken any medication known to affect bone metabolism nor presented with any prior osteoporosis fracture. The second group was scanned as part of the ASTEROID study at different locations in Canada, namely at the Shriners Hospital for Children and images were shared to our group Children-Canada. The study coordination was done by the McGill University in Montreal. This group is was composed of 35 female females and 15 male individuals leading to 50 OI diagnosed subjects. The youngest and oldest patients are 19 and 69 year old, respectively. The median age is 44.33–55 years males with confirmed diagnosis of OI Type I, III or IV. There were 35 subjects were diagnosed with type I OI patients diagnosed with OI type I, 2 with type III, and 13 with type IV. The participants of the OI group were aged between 19 and 69 years old with a mean age of 44 ± 14 years.

2.2. HR-pQCT

HR-pQCT scans (XtremeCTII, SCANCO Medical, Brüttisellen, Switzerland) were performed at the distal tibia on all patients from both groups. People of Participants in the healthy group were scanned using an in-house protocol as described in [23] whereas OI subjects were scanned using the manufacturer's standard protocol. The main differences of the in-house protocol with the manufacturer's standard protocol are the following: The reference line is. Namely, the reference line was positioned at the proximal margin of the dense structure formed by the tibia plafond instead of the subchondral endplate of the ankle joint (standard clinical section) [27]. Three and three stacks were scanned proximal to this reference line, see Figure 1a. On the other hand, participants in the OI group were scanned using the manufacturer's standard protocol i.e. the reference line instead of one stack is placed at the subchondral endplate of the ankle joint and one stack was scanned at 22.5 mm proximal to the reference line for (standard clinical section) [27].

These differences are shown) [27], see Figure 1b. The scanned region according to the two different protocol are shown side by side in Figure 1. For both group the healthy and the OI groups, each stack consist consisted of 168 voxels and a slices and a voxel resolution of 61 μm in the three principal directions which lead. This led to a thickness about of roughly 10.2 mm for each stack. Scanning settings were a Standardized scanning settings were used (voltage of 60 kVp, 900 A, 100 ms integration time) for the healthy group

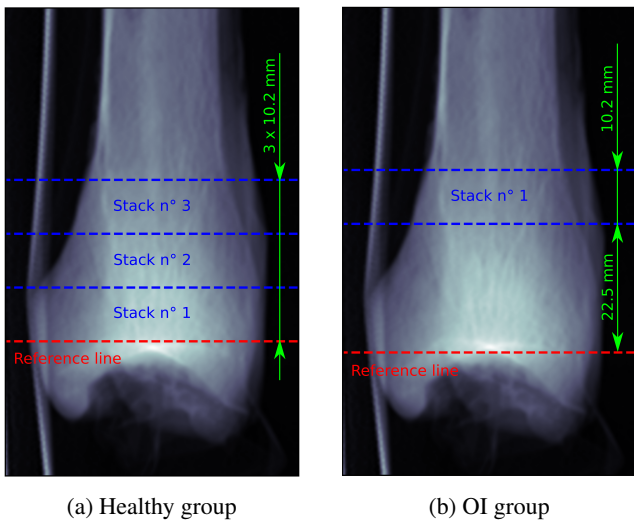


Figure 1: Clinical section scanned for both group

as well as for the OI group. For the healthy group, motion artefacts of first, middle and last slice were graded. The scale used start from (i.e slices number 1, 252, and 504) were graded on a scale of 1 (no motion artefacts) to 5 (extreme motion artefacts), as proposed by the manufacturer Pialat et al. [21]. The final grade of each scan was defined as the highest slice grade. For the OI group, as the scan consists of one stack, only one grade was attributed using the same scale as for the control group. Scans were then processed independently of their quality grading. A summary of the scans grading densities is shown in Figure 2.

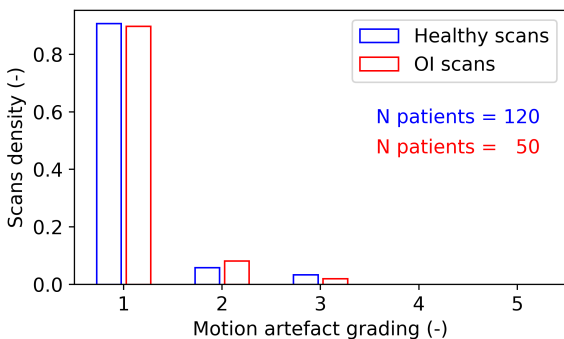


Figure 2: Summary of the motion artefacts grading. Histograms show density of each grade within both group.

2.3. Image analysis

The HR-pQCT scans were evaluated using the manufacturer's standard protocol. Briefly, an automatic contouring algorithm was applied to define the periosteal contour of the tibia (masking) and a threshold was applied for segmentation of cortical bone (450 mgHA/cm^3) and trabecular bone (320 mgHA/cm^3). Then, mask segmented images were used for further analysis.

Six ROI were randomly selected In general, six cubic ROIs were selected at random position in each scan. The conditions for ROI to be kept are no cortical bone inside and that it must be in a defined area. Each ROI had to contain trabecular bone, but no cortical bone. For the OI subjects healthy group, the ROIs were selected in the more proximal stack uniquely (see Figure 1a stack number 3) to be at the same anatomical location as for the OI group. Then for both the healthy group and the OI group, the stack was divided into two halves and the ROIs were selected to have the centers centres of three ROIs in the proximal half and three in the distal half. For the healthy people, the ROIs were selected in the more proximal stack uniquely, see Figure 1a stack n°3. As for the OI subjects, the stack is halved and centers of three ROIs were selected in both halves. One individual diagnosed with OI type III it was not possible to extract any ROI as there was no enough trabecular bone. This led to 720 healthy ROIs from 120 individuals and 294 OI ROIs from 49 individuals.

The ROI is was defined as a cube of 5.3 mm side length. This size was chosen to correspond to in agreement with the work of Panyasantisuk et al.[20] and Gross et al.[9] which , who performed similar analysis with femur μ CT scans. It was determined by Zysset et al.[29] and Daszkiewicz et al.[6] to be the optimal size to obtain accurate FEA results allow one to have a relative homogeneity of trabecular tissue within the ROI leading to accurate μ FE results with a minimal computational cost.

The After ROI cleaning, i.e. deletion of unconnected region of bone material, the morphological analysis of ROIs was performed using medtool (v4.5; Dr. Pahr Ingenieurs e.U., Pfaffstätten, Austria). The morphological parameters analyzed are: BV/TV, SMI structural model index (SMI), trabecular number (Tb.N.), trabecular thickness (Tb.Th.), trabecular spacing separation (Tb.Sp.), and the standard deviation of the trabecular spacing (Tb.Sp.SD). Moreover, ROI tissue bone mineral density (tBMD) and fabric was evaluated using MIL method [17]. The fabric tensor M was computed using mean intercept length (MIL) method [17]. It is a positive-definite second-order tensor . It is build as shown in Equation 1 below:

$$\mathbf{M} = \sum_{i=1}^3 m_i \mathbf{M}_i = \sum_{i=1}^3 m_i \mathbf{m}_i \otimes \mathbf{m}_i \quad (1)$$

where m_i are the eigenvalues of \mathbf{M} and \mathbf{M}_i are the dyadic product of the corresponding eigenvectors \mathbf{m}_i [5, 10]. The fabric is then tensor is independent of BV/TV and normalized with $tr(\mathbf{M}) = 3$. The fabric eigenvalues allow to compute the degree of anisotropy (DA) of the ROI by dividing the highest eigenvalue by the lowest one. Figure 3 shows an example of a typical ROI with the visualization of its fabric tensor.

After ROI cleaning, i.e. deletion of unconnected region of bone material, an homogenized

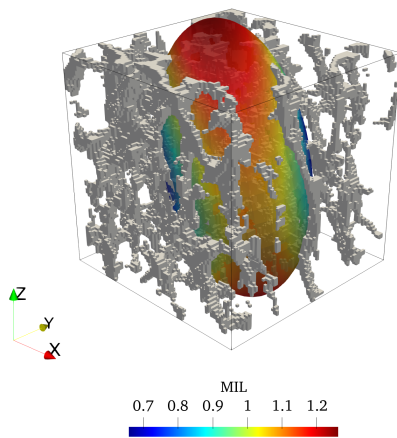


Figure 3: Typical ROI with the visualization of its fabric tensor using MIL method. Eigenvectors of the fabric tensor define its orientation and eigenvalues set lengths of the ellipsoid radii. DA is the ratio between the highest and the lowest eigenvalue.

A μFE mechanical analysis was performed using ABAQUS 6.14. Each voxel of the cleaned ROI was converted to mesh using a fully integrated linear brick elements (C3D8) with using a direct voxel conversion approach. Then, a stiffness E of 10,000 MPa and a Poisson's ratio ν of 0.3. The simulation were assigned. The homogenization process consisted of 6 independent simulations of different load cases, 3 uni-axial and 3 simple shear cases, using KUBCs. KUBCs were used according to the work of Panyasantisuk et al. kinematic uniform boundary conditions (KUBCs) [20]. Unlike PMUBCs periodicity-compatible mixed uniform boundary conditions (PMUBCs), KUBCs do not require one to rotate the ROI into fabric coordinate system which decrease the. Such rotation would potentially decrease image quality. This homogenization process allows The homogenization process allowed to calculate the components of the stiffness tensor and to calibrate the parameters of the Zysset-Curnier fabric-elasticity model [28]. This model builds the fourth order stiffness tensor \mathbb{S} using the BV/TV or ρ , fabric information tensor \mathbf{M} , three elasticity parameters λ_0 , λ_0' , and μ_0 , and two exponents, k and l . The building of this tensor is, as shown in Equation 2.

$$\begin{aligned} \mathbb{S}(\rho, \mathbf{M}) = & \sum_{i=1}^3 \lambda_{ii} \mathbf{M}_i \otimes \mathbf{M}_i \\ & + \sum_{\substack{i,j=1 \\ i \neq j}}^3 \lambda_{ij} \mathbf{M}_i \otimes \mathbf{M}_j \\ & + \sum_{\substack{i,j=1 \\ i \neq j}}^3 \mu_{ij} \mathbf{M}_i \overline{\otimes} \mathbf{M}_j \end{aligned} \quad (2)$$

With

$$\begin{aligned} \lambda_{ii} &= (\lambda_0 + 2\mu_0)\rho^k m_i^{2l} \\ \lambda_{ij} &= \lambda'_0 \rho^k m_i^l m_j^l \\ \mu_{ij} &= \mu_0 \rho^k m_i^l m_j^l \end{aligned}$$

Where \otimes and $\overline{\otimes}$ are the dyadic and symmetric product of second order tensors, respectively. To express the stiffness tensor obtained from the homogenization process with the Zysset-Curnier model, it had to be transformed into the fabric coordinate system using a coordinates transformation formula (see Equation 3) and projected onto orthotropy, leading to 12 components.

$$\mathbb{S}'_{ijkl} = Q_{im} Q_{jn} Q_{ko} Q_{lp} \mathbb{S}_{mnop} \quad (3)$$

Where \mathbb{S}' and \mathbb{S} are the transformed and the original stiffness tensor respectively and Q is the orthogonal matrix that maps the original coordinate system into the new one (fabric). The Zysset-Curnier model is built with the assumption of orthotropy and homogeneity. However, the trabecular structure is not perfectly homogeneous. In order to assess the ROI heterogeneity a so-called, a coefficient of variation (CV) is computed as presented in according to Panyasantisuk et al. [20]: the ROI is divided into eight identical subcubes, subcubes and BV/TV is computed for each subcube and the of them. The CV is defined as the ratio between the standard deviation of these BV/TV and the mean value, see Equation 4 below: (Equation 4).

$$CV = \frac{std(BV/TV_{subcubes})}{mean(BV/TV_{subcubes})} \frac{SD(BV/TV_{subcubes})}{mean(BV/TV_{subcubes})} \quad (4)$$

2.4. Statistics

The morphological parameters analyzed morphological parameters (BV/TV, Tb.N., Tb.Th., Tb.Sp., and Tb.Sp.SD, SMI, DA, and CV) were compared for both group between the healthy and the OI groups. As the initial groups do not have similar distributions of age and sex, a matching was performed by selecting similar individuals leading to identical mean and median age as well as identical gender distribution. Then, the selection of statistical test to perform was executed

~~as follow:~~ For each parameter, the median value between the six ~~ROI of ROIs from~~ the same individual was computed. The median was preferred over the mean because it is less influenced by outliers. Normality of the distribution was assessed with QQ plot and Shapiro-Wilk test. ~~If normality assumption was met, Bartlett test for equal variances was performed. Otherwise, data were log-transformed to try to achieve normal distribution. If even after log transformation, normality assumption was not met, original data space was kept and CV had to be log-transformed to meet normal distribution assumption. Then, equal variances was assessed using Bartlett test or Brown-Forsythe test was applied to assess the equal variance assumption.~~ according to the normality distribution of the data. According to the ~~previous results~~, normality and equal variances assumptions, t-test was performed if ~~normal distribution and equal variance were met~~. If only the ~~equal varianees assumption was met~~, Mann-Whitney test was preferred. Finally, if ~~none of these conditions could be assumed~~, or a non-parametric permutation test was performed. The general significance level was set to 95% for all tests. Confidence intervals ~~in means difference was~~ were computed for t-tested variables to ~~confirm p values~~ quantify the difference in both groups means. As Mann-Whitney test ~~is~~-tests are performed on the median, only ~~corresponding p value is given~~ the corresponding p-value is presented. Finally, non-parametric permutation test ~~is~~-tests are less powerful but give an empirical 95% exclusion range and a ~~p value~~ p-value. If the difference in means belong to this exclusion range, it can be stated that group means are different with 95% certainty.

2.5. Fit to model Linear Regression

The orthotropic stiffness tensors obtained ~~from the mechanical simulations were transformed into~~ after transformation onto fabric coordinate system ~~and projected onto orthotropy, leading to 12 components. The resulting orthotropic stiffness tensors~~ were then used to perform a multiple linear regression ~~on~~ with the Zysset-Curnier model. Standard linear models assume independent and identically distributed (iid) variables. As this assumption ~~is~~-was violated by the fact that six ROIs ~~are analyzed by~~ were analyzed per individual, a linear mixed-effect model was preferred. This last model, shown in Equation 5 in Laird-Ware form [13], ~~takes into account~~ considered the non-independence of ROIs from the same individual. ~~Detailed~~ A more detailed form of this model is presented in Appendix A.

$$y = X\beta + Z\delta + \epsilon \quad \text{with} \quad y = \ln(S_{rc}) \quad (5)$$

Where S_{rc} is the r th row and c th column of the non-zero element of the orthotropic stiffness tensor \mathbb{S} in Mandel notation [16], X is a $12nxp$ design matrix containing the the BV/TV and fabric info of the n ROIs and β is a $px1$ vector of fixed effects containing model parameters. Z is a $12nxf$ design matrix which contains data with individual dependence and δ is a $f \times 1$ vector composed of random factors. Finally, ϵ is a $12nx1$ vector containing the regression residuals. ~~As~~

k and l are exponents, the regression was performed on the log space.

The linear regression was performed on both group (~~healthy healthy~~ and OI) separately. To improve the fit quality, the data sets were filtered. The aim here ~~is~~-was to filter out ROIs ~~whose are too far from violating~~ the assumption of homogeneity. Therefore, analogously to the work of Panyasanitisuk et al.[20], a fixed threshold for the CV was used. To simplify comparison, we used the same value ~~of~~ 0.263 ~~was~~ fixed as exclusion criterion ~~—Besides~~[20]. Then, the relation between BV/TV and CV was assessed using Spearman's correlation coefficient. ~~Furthermore, to~~ To compare the stiffness constants (λ_0 , λ'_0 , and μ_0) between the groups, regression must be performed on identical value ranges. ~~To do this~~ Therefore, a matching was performed for BV/TV and DA to find corresponding control ~~ROI~~ ROIs for each OI in the filtered groups. Best correspondences were kept and duplicates were dropped. Finally, as the regression ~~is~~-was performed in the log space, ~~it is necessary to use identical exponent~~ slight differences in the exponents (k and l) ~~for both group~~ would lead to important variation of the stiffness constants (λ_0 , λ'_0 , and μ_0) so it was necessary to use identical exponents for both groups, weighting identically BV/TV and DA between regressions, ~~to compare stiffness constants~~. The exponents were determined by grouping healthy and OI for regression. Then a modified system ~~is~~-was used to perform the fit on separated groups, see Appendix A, Equation 12.

Another modification of the model ~~is~~-was to add a regressor for the group variable (healthy or OI), i.e. add a column to the design matrix X and a row to the parameter vector β . This modified model is compared to the original by analysis of covariance (ANCOVA) using the fixed-effects only to determine the statistical significance of the group. Implementation of this modification was performed according to [8]. A similar mixed-effect model was used to analyze the relation between tBMD and BV/TV and the significance of the group, see Appendix A Equation 14. The model used the BV/TV and the group (healthy or OI) as fixed variables and the individual as random variable. Moreover, to test the hypothesis of no interaction between the BV/TV and the group, i.e. the group has no significant influence on the tBMD versus BV/TV slope, the model was modified to add the interaction regressor (BV/TV x Group). The detailed linear systems for each model discussed here are available in Appendix A and a summary of the data sets used for the different methods is shown in Table 1.

The regression was performed using the STATSMODELS package from PYTHON 3.6. Regression quality ~~for the tBMD analysis~~ was assessed using the Pearson correlation coefficient (R^2) and the standard error of the estimate (SE). Regression on Zysset-Curnier model was assessed using the adjusted Pearson correlation coefficient squared (R^2_{adj}) and relative error between the orthotropic observed and the pre-

Table 1
Summary of the data set used for different methods

| Data sets | Original | | Age & gender matched | | CV filtered | | BV/TV & DA matched | |
|-------------------|-------------------|--------------------|----------------------|----------|-------------------|----------|--------------------|----------|
| Group Individuals | Healthy 120 | OI <i>50–49</i> | Healthy 28 | OI 28 | Healthy 119 | OI 38 | Healthy 57 | OI 32 |
| ROIs | 720 | <i>300–294</i> | 168 | 168 | 603 | 117 | 82 | 82 |
| Methods | Linear regression | | Statistics | | Linear regression | | Linear regression | |

dicted tensor using norm of fourth-order tensors (*NENE*), see Equation 6 and 7.

$$R^2_{adj} = 1 - \frac{RSS}{TSS} \frac{(12n - 1)}{(12n - p - 1)} \quad (6)$$

Where RSS is the residual sum of squares and TSS is the total sum of squares i.e. sum of the square of the observations y . n is the number of ROIs and p the number of parameters.

$$\underline{NENE} = \sqrt{\frac{(\mathbb{S}_o - \mathbb{S}_p) :: (\mathbb{S}_o - \mathbb{S}_p)}{\mathbb{S}_o :: \mathbb{S}_o}} \quad (7)$$

3. Results

3.1. Morphological Analysis

The results of the morphological analysis are summarized in Table 2. In the present study, the individual matching allowed. The individual matching for age and sex allowed us to have similar group distribution distributions with 17 females and 11 males in each group. The mean age of matched healthy individuals is $41y \pm 14$ and $41-14y$ and $41y \pm 15$ for the matched OI individuals. BV/TV of healthy people individuals is higher than BV/TV of OI group with a difference 95% CI of [0.016, 0.101] and p value p -value <0.01 . Similarly, trabecular number is higher in the matched healthy group with a compared to the matched OI group with a difference 95% CI of [0.099, 0.285] and a corresponding p value p -value <0.001 . The trabecular thickness does not show significant differences between groups with a p value of 0.2. On the other hand, trabecular spacing permutation test performed for trabecular separation showed that trabecular separation is higher in matched OI group than in matched OI group compared to healthy individuals with a p value p -value of 0.01 and an exclusion range of $(-\infty, -0.384] \cup [0.421, \infty)$. Trabecular spacing SD present to be separation SD is higher in OI patients than in matched healthy with a p value p -values <0.001 and of 0.02, respectively.

Finally, the log transformation of the coefficient of variation gives the stronger difference in means with a p value <0.0001 and a 95% CI of [0.757, 0.333] where CV is higher in matched OI individuals compared to matched healthy individuals.

In the table, Table 2 compares absolute values and p values of test statistics are compared with literature. Regarding age, the present population is slightly younger than in other study but stay in a similar range. In a general way p values of the p -values to literature. The present population age is fairly consistent with the other studies [7, 12, 22]. The three other studies, Folkestad et al.[7], Kocjan et al.[12], and Rolvien et al. [22], show significant differences for BV/TV, Tb \bar{N} , Tb \bar{Sp} , N., Tb \bar{Sp} , and Tb \bar{Sp} SD and no significant differences for Tb \bar{Th} . Absolute Th. In the present study, absolute values of BV/TV, TB \bar{Th} , Tb \bar{Sp} , Tb \bar{Sp} .Th., Tb \bar{Sp} , and Tb \bar{Sp} SD are higher in the present study. Sp.SD seem to be higher compared to literature. On the other hand, Tb \bar{N} .N. appears to be higher in the other studies than in the present one lower compared to studies in literature [7, 12, 22].

3.2. Linear RegressionsRegression with Original Data Sets

Figure 4 shows the result of regression for complete data sets results of the linear regression analysis of each group separately. The x-axis represent, between the values of observed tensors from mechanical simulations. The y axis is the observed stiffness tensors from μFE simulations and the predicted values using the Zysset-Curnier model[28] and the parameters obtained after performing the regression with linear mixed-effect model. The fitted line is represented by the dashed line. λ_{ii} stands for the diagonal terms of normal components of \mathbb{S} in Mandel notation[16], λ_{ij} for the off-diagonal terms of normal components, and μ_{ij} for the shear components, indicating the theoretical perfect correlation. For the healthy group, see Figure 4a, (Figure 4a) the fit is performed on 720 ROIs leading to 8640 data points. The R^2_{adj} is slightly above 0.95 and the NE is of $18\% \pm 10\%$. The regression of analysis for the OI group could only be (Figure 4b) performed on 294 ROIs as it was not possible to find suitable ROIs for one patient. Nevertheless, it leads to 3528 points, a data points, an R^2_{adj} close to 0.85 and a NE of $62\% \pm 233\%$. It can be noticed that, as the values of observed the observed stiffness tensor decreases, points tends data points tend to be further apart of from the diagonal (dashed line). Moreover,

Table 2: Summary of the tibia ROIs morphological analysis and comparison with literature. Values are presented as mean \pm standard deviation when statistical test is performed on the means or median (inter-quartile range) when test is on medians. The study of [12] presents n.s. for non-significant p value test result.

| Variable | Group | Present study | | | Folkestad et al.[7] | | | Kocijan et al.[12] | | | Rolvien et al.[22] | | |
|----------|-----------|----------------------|---------|------------------|---------------------|----------------------|---------|--------------------|---------|--------|--------------------|--------|---------|
| | | Values | p value | Values | p value | Values | p value | Values | p value | Values | p value | Values | p value |
| Age | Healthy | 41 \pm 14 | | 54 (21-77) | | 44 (38-52) | | 49 \pm 16 | | | | | |
| | OI Type I | 41 \pm 15 | | 53 (21-77) | | 42 (35-56) | | 46 \pm 16 | | | | | |
| BV/TV | Healthy | 0.222 \pm 0.081 | <0.01 | 0.14 \pm 0.03 | <0.001 | 0.141 (0.130-0.170) | | 0.162 \pm 0.010 | <0.0001 | | | | |
| | OI Type I | 0.164 \pm 0.079 | | 0.08 \pm 0.03 | | 0.098 (0.088-0.114) | | 0.095 \pm 0.008 | <0.0001 | | | | |
| Tb.N. | Healthy | 0.842 \pm 0.144 | <0.001 | 1.94 (1.74-2.13) | <0.001 | 1.76 (1.59-2.08) | | 2.143 \pm 0.089 | <0.0001 | | | | |
| | OI Type I | 0.650 \pm 0.198 | | 1.30 (0.75-1.53) | | 1.33 (1.07-1.55) | | 1.428 \pm 0.098 | <0.0001 | | | | |
| Tb.Th. | Healthy | 0.301 (0.287-0.321) | 0.2 | 0.07 (0.06-0.08) | 0.5 | 0.081 (0.074-0.087) | | 0.075 \pm 0.003 | 0.046 | | | | |
| | OI Type I | 0.306 (0.292-0.331) | | 0.07 (0.06-0.08) | | 0.074 (0.064-0.090) | | n.s. | | | | | |
| Tb.Sp. | Healthy | 0.924 \pm 0.257 | 0.01 | 0.44 (0.39-0.51) | <0.001 | - | | 0.409 \pm 0.023 | 0.0003 | | | | |
| | OI Type I | 1.422 \pm 0.694 | | 0.68 (0.57-1.19) | | - | | 0.727 \pm 0.095 | | | | | |
| Tb.Sp.SD | Healthy | 0.317 \pm 0.136 | 0.02 | 0.20 (0.16-0.25) | <0.001 | 0.2221 (0.170-0.242) | | - | | | | | |
| | OI Type I | 0.631 \pm 0.383 | | 0.40 (0.31-1.11) | | 0.382 (0.311-0.504) | | <0.0001 | | | | | |
| SMI | Healthy | 0.001 (-0.021-0.033) | <0.001 | - | | 0.698 (0.511-0.890) | | <0.001 | | | | | |
| | OI Type I | 0.056 (0.015-0.079) | | - | | - | | - | | | | | |
| DA | Healthy | 1.992 (1.826-2.020) | 0.02 | - | | - | | - | | | | | |
| | OI Type I | 2.018 (1.901-2.158) | | - | | - | | - | | | | | |
| ln(CV) | Healthy | -1.723 \pm 0.344 | <0.0001 | - | | - | | - | | | | | |
| | OI Type I | -1.178 \pm 0.441 | | - | | - | | - | | | | | |

data the points from the points coming from the stiffness tensors with lowest values are only exclusively above the diagonal. One last observation which should be noted is the range covered by the observed tensors. The range of stiffness tensors of the OI group is wider than compared to the one of the healthy group and ROIs with lower BV/TV present further low lower stiffness values. The values of these ROIs stiffness tensors components tends to be overestimated by the fit.

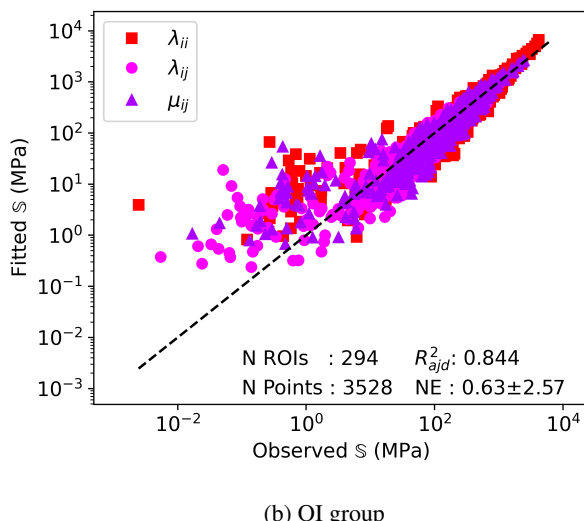
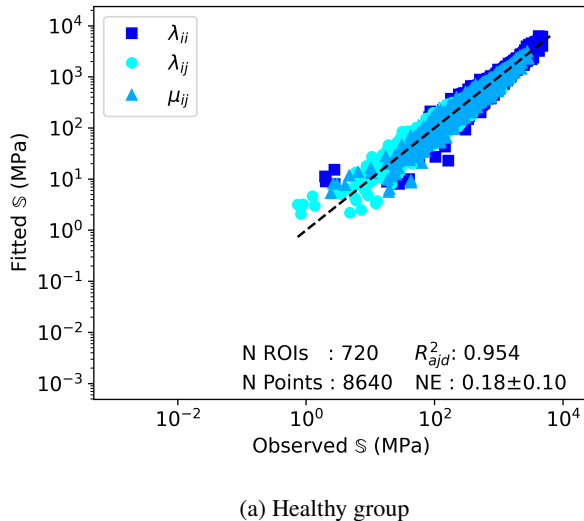


Figure 4: Regression results using the fixed effects of the linear mixed-effect model on original data sets. λ_{ii} stands for the diagonal terms of normal components of \mathbb{S} in Mandel notation[16], λ_{ij} for the off-diagonal terms of normal components, and μ_{ij} for the shear components. The dashed line represents the fitted line.

3.3. Filtering

The CV in relation to BV/TV is shown in Figure 5. The OI data reach higher values of CV and stay at lower values

of reached higher CV values and lower BV/TV than-values compared to healthy data. Generally, the CV tends to increase with decreasing BV/TV. The Spearman coefficient is shown above the plot as value [95% CI]. Its value is negative and strictly different from zero. Finally, the CV threshold value used to filter the data is represented by the dashed line. It can be observed that a relatively important part of OI data will be filtered out. On the other hand, relatively few healthy data will be removed by the filtering. Examples gets removed. 3D representation of extreme ROIs in terms of CV and BV/TV are shown in Appendix B.

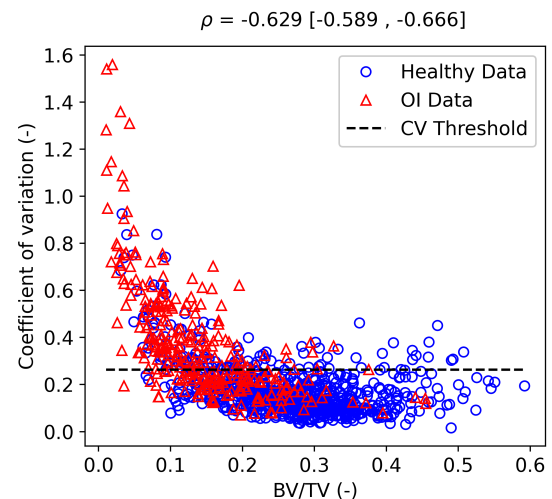


Figure 5: Coefficient of variation in relation to BV/TV. Spearman correlation coefficient ρ assess monotonic relation between two variable

The regression results of the filtered data are presented in Figure 6. After filtering, healthy group is the healthy group was reduced to 119 individuals and 603 ROIs. This leads to resulting in 7236 points for the regression. Results shown similar values as for the complete data set, namely a data points, an R^2_{adj} close to 0.95 and a NE of $16\% \pm 8\%$, see Figure 6a. The OI group lost more individuals after filtering (Figure 6a). In the OI group, more individuals were filtered leading to 38 people and 115 ROIs. Regression is performed on, and 1380 points then. Figure 6b presents results with a data points (Figure 6b). This resulted in an R^2_{adj} rounded close to 0.95 and a NE of $17\% \pm 8\%$.

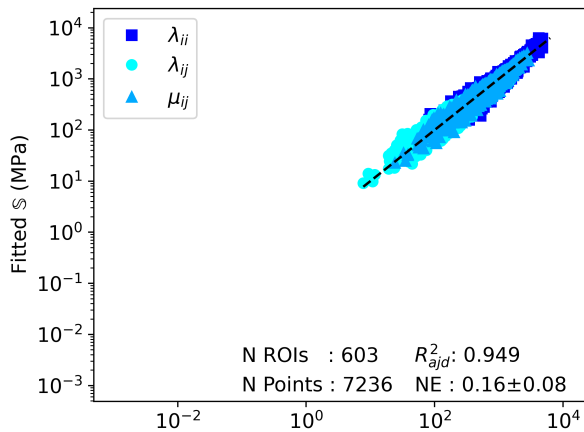
3.4. BV/TV and DA Matching

Regression results after BV/TV & and DA ROI matching are shown in Table 3. The columns show which data set was used the used data set, the five parameters of the Zysset-Curnier model (λ_0 , λ'_0 , μ_0 , k , and l) and the assessment of fit quality (R^2_{adj} and NE). Grouping healthy and OI data together for regression lead to a k of 1.91 and a l of 0.95. Regression result shows a R^2_{adj} of 0.94 and a NE of $18\% \pm 9\%$. Second and last rows The second and the last row show regression results using separated data sets and imposing the

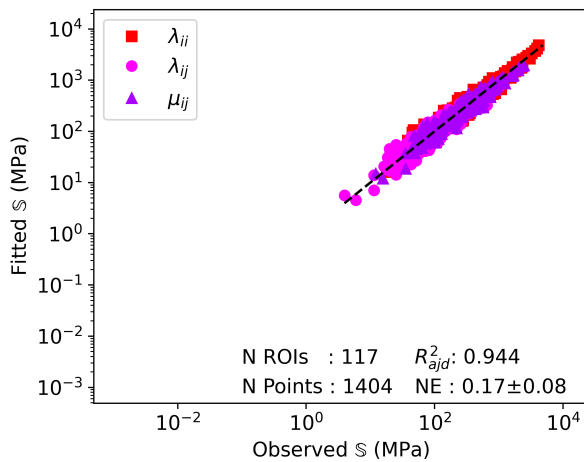
constants for the observed data set than for compared to the other studies [9, 20].

4. Discussion

The age of matched individuals lies in the spectrum of the others studies which allow to compare the morphological values. The main explanation for The analysis of tBMD in relation to BV/TV is shown in Figure 7. The t-test performed on the tBMD distributions led to a p-value <0.0001 and a 95% CI of [-35,-13]. The linear regression performed using the linear mixed-effects model without BV/TV and group interaction provided a slope of 223 [153,292] (value [95% CI]). The intercept value was 534 [518,550] and the group variable led to a value of 14 [7,20]. The prediction using the fixed effects only led to a R^2 of 0.23 and a SE of 33. Then, using the linear mixed-effect model with the interaction regressor (BV/TV x Group), this added variable presented a value of 3 [-66,72] and a p-value of 0.94.



(a) Healthy group



(b) OI group

Figure 6: Regression results using the fixed effects of the linear mixed-effect model on filtered data sets. λ_{ii} stands for the diagonal terms of normal components of \mathbb{S} in Mandel notation[16], λ_{ij} for the off-diagonal terms of normal components, and μ_{ij} for the shear components. The dashed line represents the fitted line.

exponents k and l -OI values to fixed values. OI stiffness constants (λ_0 , λ'_0 , and μ_0) are higher than healthy one. The increase is of 15%, 1%, and 2% for λ_0 , λ'_0 , and μ_0 , respectively. The ANCOVA performed to quantify the group statistical significance shows a p value of 0.7.

Table 4 shows results obtained compared to literature. Gross et al. [9] has the larger number of ROIs. Data sets of Panyasantisuk et al. [20] show BV/TV ranges slightly higher than in the present study and the one of Gross et al. [9]. On the other hand, DA is higher in the present study than for Panyasantisuk et al. [20] and Gross et al. [9]. Setting the exponents k and l to the same values lead to lower stiffness

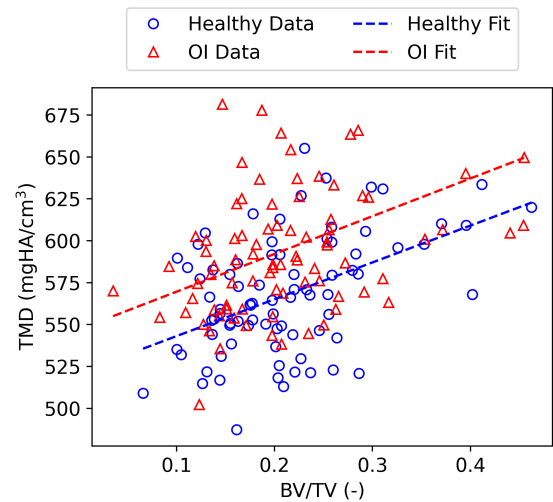


Figure 7: tBMD in relation to BV/TV. The fitted lines are obtained using the fixed effects of the linear mixed-effect model and fixing the group variable.

4. Discussion

Osteogenesis imperfecta is an inherited form of bone fragility with a severity going from mild to perinatally lethal. This study aim to confirm that fabric-elasticity relationships in OI trabecular bone are similar than in healthy conditions, encouraging the use of HR-pQCT scans for fracture risk assessment. To do this, the study included two groups of participants composed of 120 healthy control and 50 OI diagnosed patients respectively.

As the previous studies [7, 12, 22] have the same age range as our matched groups, we can compare morphological parameters. The imaging system explains most of the differences between the absolute morphological values of the present

Table 3

Constants obtained with BV/TV and DA matched data sets. Comparison is performed between grouped (N ROIs = 166) and separated data sets (N ROIs = 83). Values are presented as value [95% CI] or mean \pm standard deviation. Values in gray were imposed in the regression.

| Data set | λ_0 | λ'_0 | μ_0 | k | l | R^2_{adj} | NE (%) |
|----------|------------------|------------------|------------------|------------------|------------------|-------------|---------|
| Grouped | 4626 [3892-5494] | 2695 [2472-2937] | 3541 [3246-3862] | 1.91 [1.86-1.95] | 0.95 [0.93-0.97] | 0.936 | 19 ± 9 |
| Healthy | 4318 [3844-4851] | 2685 [2533-2845] | 3512 [3306-3731] | 1.91 | 0.95 | 0.835 | 21 ± 10 |
| OI | 4983 [4345-5716] | 2727 [2547-2921] | 3600 [3355-3863] | 1.91 | 0.95 | 0.860 | 20 ± 10 |

Table 4

Comparison with literature. N stands for the number of ROIs observed. Values are presented as computed value only or mean \pm standard deviation. The present study shows values obtained with ROIs of tibia XCTII scans of healthy and OI individuals pooled together. Panyasantisuk et al. [20] and Gross et al. [9] show values obtained with ROIs of femur μ CT scans of healthy individuals only. Values in gray were imposed in the regression.

| Data set | N | BV/TV | DA | λ_0 | λ'_0 | μ_0 | k | l | R^2_{adj} | NE (%) |
|---------------------------|------|-----------------|-----------------|-------------|--------------|---------|------|------|-------------|--------------|
| Filtered data sets | | | | | | | | | | |
| Panyasantisuk et al. [20] | 126 | 0.27 ± 0.08 | 1.57 ± 0.18 | 3306 | 2736 | 2837 | 1.55 | 0.82 | 0.984 | 8 ± 3 |
| Present study | 720 | 0.27 ± 0.09 | 1.94 ± 0.24 | 2507 | 1620 | 2052 | 1.55 | 0.82 | 0.832 | 21 ± 11 |
| | 720 | 0.27 ± 0.09 | 1.94 ± 0.24 | 4778 | 3087 | 3911 | 1.99 | 0.85 | 0.949 | 17 ± 9 |
| Non-filtered data sets | | | | | | | | | | |
| Panyasantisuk et al. [20] | 167 | 0.25 ± 0.08 | 1.54 ± 0.20 | 3841 | 3076 | 3115 | 1.60 | 0.99 | 0.983 | 14 |
| Gross et al. [9] | 264 | 0.19 ± 0.10 | 1.67 ± 0.34 | 4609 | 3692 | 3738 | 1.60 | 0.99 | 0.981 | 14 |
| Present study | 1014 | 0.23 ± 0.11 | 1.94 ± 0.26 | 2738 | 1662 | 2187 | 1.60 | 0.99 | 0.622 | 40 ± 177 |
| | 1014 | 0.23 ± 0.11 | 1.94 ± 0.26 | 5020 | 3047 | 4010 | 1.98 | 0.91 | 0.916 | 30 ± 113 |

study compared to the others ~~lies in the imaging system~~. Folke et al.[7], Kocjan et al.[12], and Rolvien et al.[22] have performed ~~first generation Xtreme CT scans and the present study use image from XCTH~~ their measurements on first generation XCT scanners with a voxel size of $82 \mu\text{m}$, while we have used a second generation XCT with a voxel size of $61 \mu\text{m}$. The work from Agarwal et al.[1] investigated differences between the two scanner types. They showed that BV/TV, Tb_{Th.Th.}, and Tb_{Sp is Sp.} are higher in second generation ~~Xtreme CT and, on the other hand, TbN is higher in first generation Xtreme CT~~ scanners and Tb.N. is lower compared to first generation XCT. These results give confidence ~~on the in our~~ observed values. Another bias is introduced by the fact that the present study analyses the median values of six cubic ROIs with 5.3 mm side length. This conditions the Tb.N and Tb.Sp.N. and Tb.Sp. as they depend on the ROI size. Moreover, conditions imposed for ~~ROI random~~ random ROI selection can lead to further biased values, ~~specially of OI patient, as it can not be empty especially for OI patients, as the ROI must contain a portion of trabecular bone. The CV presenting the stronger significant difference between groups even given the low sample size~~ Even with the low sample size (2x28 individuals), the statistic tests have shown significant differences between groups with the more significant being for the CV values. The CV values show that heterogeneity ~~is a main difference in OI patient of OI trabecular bone is higher compared to healthy individuals~~ control and the more discriminant parameter. Fi-

ndnally, the significant differences observed in BV/TV and DA even with ~~age & gender matched individuals justify~~ matched age and gender justifies the choice of a variable matching for fabric-elasticity relationships analysis, because the fit must be performed on identical ranges to obtain comparable values.

Regression performed The linear regressions performed in this study on original data sets shows showed R^2_{adj} and NE in the expected range (i. e. slightly lower than Gross et al. [9] and Panyasantisuk et al.[20]) for the healthy group. Components of the stiffness tensors are distributed to both sides of the diagonal. On the other hand, regression of the OI the linear regressions performed in this study using the OI original data set presents lower R^2_{adj} and higher NE than such fit reach usually [9, 20]. The important value of NE and its standard deviation shows that the fitted stiffness can deviate significantly from the observation. These differences come from the ROIs presenting a low stiffness. It can be seen on the regression plot The regression plot (Figure 4b) shows that when the stiffness term decreases about decreases to 10^0 and under MPa and lower, the fit tends to overestimate the stiffness. This is due to the fact that because ROI stiffness is highly impacted by dependent on BV/TV. Some values. Some ROIs with low BV/TV ROIs do not don't have every side of the cube connected by bone, leading to extremely low terms in the stiffness tensor, see Appendix B. Trying to homogenize such ROI ROIs can lead to error errors of

multiple order of magnitude, as observed on the plot (Figure 4b). Therefore, a filtering is indispensable to assess and compare fabric-elasticity relationships, as done by Panyasantisuk et al. [20]. An alternative of CV filtering to CV filtering for assessing the ROI heterogeneity could be to compute the area ratio proportion of the area filled by bone on each of the six faces of the ROI to assess the ROI heterogeneity.

Figure 5 presenting presents the CV in relation to BV/TV that there is. It shows a tendency of CV values to increase with a decreasing BV/TV values. Effectively, if the quantity of material inside the ROI decreases, the distribution homogeneity of this mass is more sensitive and therefore can quickly becomes become highly heterogeneous. A simple assumption about this relation is that it could be monotonic. Pearson's correlation coefficient being strictly negative confirms a negative monotonic relation. As some ROIs with higher BV/TV ROIs still present high CV values, imposing a fixed threshold make sense for subsequent homogenization seem feasible. However, the value of this threshold actually results from an optimization process in the study of Panyasantisuk et al.[20] and could be subject to more investigations.

The fits linear regressions performed on filtered data sets present direct effect of filtering as the ROIs meeting the homogeneity assumption lead to better results compared to linear regression including ROIs with high CV values. For the healthy group (N=603), the relatively small decrease of R^2_{adj} (5%) compared to the linear regression using the unfiltered data set is negligible. On the other hand, NE presents an improved value decreasing values are decreased by 2%. These results are due to the filtering of point and therefore improved. The filtering eliminates data points further away from the diagonal (better NE) and some other data points close to the diagonal leading to a smaller number of points (modifying R^2_{adj}). For the OI group, filtering leads to an important improvement of the fit. Results become similar to the healthy group in terms of linear regression (i.e. higher R^2_{adj} and lower NE). R^2_{adj} , NE, and the range of stiffness values are almost at the level of the healthy group. These results give confidence to the filtering procedure and are a first step to in accepting the hypothesis of no different fabric-elasticity relationships between healthy and OI trabecular bone having the same fabric-elasticity relationships.

After BV/TV and DA matching, grouping the data sets together lead led to similar R^2_{adj} and NE as for the individual filtered data sets. This allows to give one to determine values for k and l for the tibia at a spatial resolution of 61 μm . Imposing these values to perform the fit on individual match data set allow linear regression on data sets of the matched individuals allows us to highlight differences, if any, between healthy and OI trabecular bone. The relatively low differences for λ'_0 and μ_0 once again provide arguments for similar relationships between the two groups supports the hypothesis for similar fabric-elasticity relationships between healthy

and OI trabecular bone. For λ'_0 , this relative difference being higher could rise some doubts about this similarity but, but the 95% CI intervals still show a common range which almost include both the λ'_0 of OI and healthy linear regressions. Moreover, ANCOVA performed comparing the original formulation and the one with addition of a regressor for the group shown a p value showed a p-value far above the 5% significance level. With this statistical non-significance of the group and groups and their low relative differences in the computed stiffness constants, it can be stated that: if trabecular bone is homogeneous enough, there is no reason to suppose assume differences in fabric-elasticity relationships between healthy and OI trabecular bone. In FEA simulations, it is not possible to exclude part of the mesh because of high heterogeneity. Nevertheless, the error created by such ROIs are is negligible as this concerns ROIs with extremely low stiffness leading to a minor impact on the full model.

Imposing k and l allows one to estimate the effect of different image resolutions. Panyasantisuk et al.[20] and Gross et al.[9] both used femur scans with 18 μm spatial resolution and coarsened it them to 36 μm . Gross et al.[9] showed that different anatomical locations lead to only slight differences. Comparing regression of the filtered data set of Panyasantisuk et al.[20] with the present study, the lower stiffness constants observed can be explained partially by the higher DA range and by the coarser resolution. Differences of R^2_{adj} and NE come from the imposition of k and l to a different value than the optimal ones. Then, comparing regression results of Panyasantisuk et al.[20], Gross et al.[9], and the present study, BV/TV ranges stay overlapped overlap. As for the filtered data sets, DA is higher in the present study and the stiffness constants remain lower than for the two other studies. Here, differences in DA can mainly be explained by the different anatomical location and differences in stiffness constants by resolutions as a result of the different image resolutions. The distal tibia, unlike the proximal femur, is mainly loaded in one direction which explain explains this increase of DA. Lower stiffness constants are obtained because the coarser structure resulting from XCTII cannot't be as optimized as the fine detailed structure obtained by μCT . Effectively, the architecture resulting from μCT scans can reproduce the optimized morphology of trabecular bone with a high fidelity. By decreasing the scan spatial resolution, the scanned structure becomes more bulky bulkier. Performing a fit linear regression on this less optimized structure lead leads to the observed lower stiffness constants. Finally, the comparison between R^2_{adj} and NE of current study without imposing k and l and the ones of Panyasantisuk et al.[20] and Gross et al.[9] show shows that lower spatial resolution lead leads to lower fit quality. Nevertheless, l stands stays in the same range as for the two other studies [9, 20], meaning the relative weight of DA remains constant. On the other hand, the higher k highlight highlights an increased relative weight of BV/TV.

The analysis of tBMD gives interesting outputs as well.

Although BV/TV and DA are in the same range because of the matching, the t-test reveal a higher tBMD in OI trabecular bone than in healthy condition with 95% certainty and a very high significance level. The coefficients obtained from the linear mixed-effects model show that there is a relation between tBMD and BV/TV as zero is not included in the slope CI. This result can have different origins. From a biological point of view, the remodeling process leads to a mineralization gradient from the core of the trabecula to the outer surface. As trabecular thickness decreases with BV/TV, this means that with a lower BV/TV the core of trabeculae could be less mineralized. The second explanation for this slope comes from the scanning. Effectively, during scanning a phenomenon called partial volume effect occurs and its impact decreases with an increasing BV/TV. Nevertheless, the former (biological) explanation is expect to have a less significant impact than the latter (scanning). Regarding the other coefficients of the linear regression, the CI of group variable exclude zero as well leading to the conclusion that we have 95% certainty that the intercept is different depending on the group. This could be explained by the bisphosphonate treatment that OI patients receive. Effectively, bisphosphonate is aimed to freeze the remodeling process which lead to higher mineralization of the bone. According to the results of Indermaur et al.[11] these findings suggest to add a correction accounting for the tBMD in FE simulations to catch the higher modulus, ultimate stress and post-yield behavior of OI bone compared to healthy bone at the ECM level. Regarding the interaction between BV/TV and the group, the p-value obtained show a high non-significance meaning that the slopes of both OI and healthy groups are the same. This could be visualized in Figure 7 where the fitted lines are obtained using the fixed effects of the model and the group variable if fixed. In this plot, performed with the interaction term (BV/TV x Group) the fitted lines appear to be quasi-parallel.

The main limitations of this study are the definition of "homogeneous enough" and the fact that it is limited to tibiae XCTII scans. Moreover, having only one patient with OI type III where we could extract ROIs does not allows to do statistics. Effectively as those patients are in wheelchair, it could be interesting to analyze the impact of this condition on the weight bearing tibia. The ROI homogeneity has an important impact on the analysis quality. As proposed earlier, ROI homogeneity could be assessed in another way to be able to propose a more precise ROI filtering for fitting. More investigations could be performed to improve the model for highly heterogeneous ROIs, but as it concerns mainly ROI with low stiffness the impact on FEA models ~~can be negligible~~. Similar could be negligible if the proportion of such low stiffness ROIs stays low. A similar study could be performed ~~using~~ on XCTII radii scans to confirm the low differences between anatomical locations for coarser resolution. Another limitation is that the scans were performed on different devices which were not cross-calibrated. However, as they are the same model, it is expected to have a minor impact.

In conclusions, the ~~sample~~ samples analyzed in the ~~this study have similar morphology that present study had similar morphology compared to data reported in the literature. We find no couldn't find~~ differences in fabric-elasticity relationships between healthy and OI trabecular bone ~~if the ROI is homogeneous enough~~, when the ROIs were homogeneous enough i.e. with a CV lower than 0.263. Indermaur et al.[11] ~~shown that compressive behavior~~ could show that the compressive behaviour of OI bone tissue is similar to ~~healthy control~~. If the one of healthy control at the ECM level. If the tensile and shearing behaviors agree behaviour is similar as well, fabric-strength relationships will hold too. Therefore, OI ~~bone fragility might mostly result from trabecular bone~~ can explain part of the bone fragility by the decrease in BV/TV and the loss of homogeneity in its trabecular organization.

Acknowledgments

The authors acknowledge Christina Wapp from the ARTORG Center for Biomedical Engineering Research for her contribution to the building and interpretation of linear mixed-effect model and Mereo BioPharma for sharing the tibia XCTII scans of OI individuals. This work was internally funded by the ARTORG Center for Biomedical Engineering Research and Mereo BioPharma. Bettina M. Willie is supported by the Shriners Hospital for Children and the FRQS Programme de bourses de chercheur.

A. Linear Models

The standard linear model has the form:

$$\ln(S_{rc}) = X\beta + \epsilon \quad (8)$$

Where ϵ is the vector of residuals. For one ROI, the system take the following form:

$$\ln \begin{pmatrix} S_{11} \\ S_{12} \\ S_{13} \\ S_{21} \\ S_{22} \\ S_{23} \\ S_{31} \\ S_{32} \\ S_{33} \\ S_{44} \\ S_{55} \\ S_{66} \end{pmatrix} = \begin{pmatrix} 1 & 0 & 0 & \ln(\rho) & \ln(m_1^2) \\ 0 & 1 & 0 & \ln(\rho) & \ln(m_1 m_2) \\ 0 & 1 & 0 & \ln(\rho) & \ln(m_1 m_3) \\ 0 & 1 & 0 & \ln(\rho) & \ln(m_2 m_1) \\ 1 & 0 & 0 & \ln(\rho) & \ln(m_2^2) \\ 0 & 1 & 0 & \ln(\rho) & \ln(m_2 m_3) \\ 0 & 1 & 0 & \ln(\rho) & \ln(m_3 m_1) \\ 0 & 1 & 0 & \ln(\rho) & \ln(m_3 m_2) \\ 1 & 0 & 0 & \ln(\rho) & \ln(m_3^2) \\ 0 & 0 & 1 & \ln(\rho) & \ln(m_2 m_3) \\ 0 & 0 & 1 & \ln(\rho) & \ln(m_3 m_1) \\ 0 & 0 & 1 & \ln(\rho) & \ln(m_1 m_2) \end{pmatrix} \begin{pmatrix} \ln(\lambda^*) \\ \ln(\lambda'_0) \\ \ln(\mu_0) \\ k \\ l \end{pmatrix} + \begin{pmatrix} \epsilon_1 \\ \epsilon_2 \\ \epsilon_3 \\ \epsilon_4 \\ \epsilon_5 \\ \epsilon_6 \\ \epsilon_7 \\ \epsilon_8 \\ \epsilon_9 \\ \epsilon_{10} \\ \epsilon_{11} \\ \epsilon_{12} \end{pmatrix} \quad (9)$$

Where $\lambda^* = \lambda_0 + 2\mu_0$. Then, the mixed-effect model, which handles multiple measurement on the same individual, has the following general form:

$$\ln(S_{rc}) = X\beta + Z\delta + \epsilon \quad (10)$$

Where Z is a design matrix composed of the observations which are correlated on the same individual and, in general, is a subset of X . In the present case, the stiffness variables (λ_0 , λ'_0 , and μ_0) can vary between individuals but the hypothesis is that they all vary by an identical factor. Therefore, the design matrix Z is composed of the addition of the three first columns of X and the system for one ROI takes the following form:

$$\ln \begin{pmatrix} S_{11} \\ S_{12} \\ S_{13} \\ S_{21} \\ S_{22} \\ S_{23} \\ S_{31} \\ S_{32} \\ S_{33} \\ S_{44} \\ S_{55} \\ S_{66} \end{pmatrix} = \begin{pmatrix} 1 & 0 & 0 & \ln(\rho) & \ln(m_1^2) \\ 0 & 1 & 0 & \ln(\rho) & \ln(m_1 m_2) \\ 0 & 1 & 0 & \ln(\rho) & \ln(m_1 m_3) \\ 0 & 1 & 0 & \ln(\rho) & \ln(m_2 m_1) \\ 1 & 0 & 0 & \ln(\rho) & \ln(m_2^2) \\ 0 & 1 & 0 & \ln(\rho) & \ln(m_2 m_3) \\ 0 & 1 & 0 & \ln(\rho) & \ln(m_3 m_1) \\ 0 & 1 & 0 & \ln(\rho) & \ln(m_3 m_2) \\ 1 & 0 & 0 & \ln(\rho) & \ln(m_3^2) \\ 0 & 0 & 1 & \ln(\rho) & \ln(m_2 m_3) \\ 0 & 0 & 1 & \ln(\rho) & \ln(m_3 m_1) \\ 0 & 0 & 1 & \ln(\rho) & \ln(m_1 m_2) \end{pmatrix} \begin{pmatrix} \ln(\lambda^*) \\ \ln(\lambda'_0) \\ \ln(\mu_0) \\ k \\ l \end{pmatrix} + \begin{pmatrix} 1 \\ 1 \\ 1 \\ 1 \\ 1 \\ 1 \\ 1 \\ 1 \\ 1 \\ 1 \\ 1 \\ 1 \end{pmatrix} (\delta) + \begin{pmatrix} \epsilon_1 \\ \epsilon_2 \\ \epsilon_3 \\ \epsilon_4 \\ \epsilon_5 \\ \epsilon_6 \\ \epsilon_7 \\ \epsilon_8 \\ \epsilon_9 \\ \epsilon_{10} \\ \epsilon_{11} \\ \epsilon_{12} \end{pmatrix} \quad (11)$$

As the linear regression is performed in the log space, it is necessary to impose the exponent k and l in order to compare the stiffness values between groups. The system is

then modified as follow:

$$\ln \begin{pmatrix} S_{11} \\ S_{12} \\ S_{13} \\ S_{21} \\ S_{22} \\ S_{23} \\ S_{31} \\ S_{32} \\ S_{33} \\ S_{44} \\ S_{55} \\ S_{66} \end{pmatrix} - \begin{pmatrix} \ln(\rho) & \ln(m_1^2) \\ \ln(\rho) & \ln(m_1 m_2) \\ \ln(\rho) & \ln(m_1 m_3) \\ \ln(\rho) & \ln(m_2 m_1) \\ \ln(\rho) & \ln(m_2^2) \\ \ln(\rho) & \ln(m_2 m_3) \\ \ln(\rho) & \ln(m_3 m_1) \\ \ln(\rho) & \ln(m_3 m_2) \\ \ln(\rho) & \ln(m_3^2) \\ \ln(\rho) & \ln(m_2 m_3) \\ \ln(\rho) & \ln(m_3 m_1) \\ \ln(\rho) & \ln(m_1 m_2) \end{pmatrix} \begin{pmatrix} k \\ l \end{pmatrix} = \begin{pmatrix} 1 & 0 & 0 \\ 0 & 1 & 0 \\ 0 & 1 & 0 \\ 0 & 1 & 0 \\ 1 & 0 & 0 \\ 0 & 1 & 0 \\ 0 & 1 & 0 \\ 0 & 1 & 0 \\ 1 & 0 & 0 \\ 0 & 0 & 1 \\ 0 & 0 & 1 \\ 0 & 0 & 1 \end{pmatrix} \begin{pmatrix} \epsilon_1 \\ \epsilon_2 \\ \epsilon_3 \\ \epsilon_4 \\ \epsilon_5 \\ \epsilon_6 \\ \epsilon_7 \\ \epsilon_8 \\ \epsilon_9 \\ \epsilon_{10} \\ \epsilon_{11} \\ \epsilon_{12} \end{pmatrix} + \ln \begin{pmatrix} \lambda^* \\ \lambda'_0 \\ \mu_0 \end{pmatrix} \quad (12)$$

Finally, a modification of the model is to add a regressor for the group variable. Using a grouped data set (healthy and OI), it allows to determine if the group is statistically significant using ANCOVA. In such case the system is written under the form:

$$\ln \begin{pmatrix} S_{11} \\ S_{12} \\ S_{13} \\ S_{21} \\ S_{22} \\ S_{23} \\ S_{31} \\ S_{32} \\ S_{33} \\ S_{44} \\ S_{55} \\ S_{66} \end{pmatrix} = \begin{pmatrix} 1 & 0 & 0 & \ln(\rho) & \ln(m_1^2) & S_g \\ 0 & 1 & 0 & \ln(\rho) & \ln(m_1 m_2) & S_g \\ 0 & 1 & 0 & \ln(\rho) & \ln(m_1 m_3) & S_g \\ 0 & 1 & 0 & \ln(\rho) & \ln(m_2 m_1) & S_g \\ 1 & 0 & 0 & \ln(\rho) & \ln(m_2^2) & S_g \\ 0 & 1 & 0 & \ln(\rho) & \ln(m_2 m_3) & S_g \\ 0 & 1 & 0 & \ln(\rho) & \ln(m_3 m_1) & S_g \\ 0 & 1 & 0 & \ln(\rho) & \ln(m_3 m_2) & S_g \\ 1 & 0 & 0 & \ln(\rho) & \ln(m_3^2) & S_g \\ 0 & 0 & 1 & \ln(\rho) & \ln(m_2 m_3) & S_g \\ 0 & 0 & 1 & \ln(\rho) & \ln(m_3 m_1) & S_g \\ 0 & 0 & 1 & \ln(\rho) & \ln(m_1 m_2) & S_g \end{pmatrix} \quad (13)$$

$$\begin{pmatrix} \ln(\lambda^*) \\ \ln(\lambda'_0) \\ \ln(\mu_0) \\ k \\ l \\ \ln(\beta_{S_g}) \end{pmatrix} + \begin{pmatrix} \epsilon_1 \\ \epsilon_2 \\ \epsilon_3 \\ \epsilon_4 \\ \epsilon_5 \\ \epsilon_6 \\ \epsilon_7 \\ \epsilon_8 \\ \epsilon_9 \\ \epsilon_{10} \\ \epsilon_{11} \\ \epsilon_{12} \end{pmatrix}$$

Where S_g is coded using a summation constraint [8], meaning, $S_g = -1$ for the healthy group and $S_g = 1$ for the OI group. This model is adapted into a linear mixed-effect model to analyze the relation between tBMD and BV/TV and the effect of the group.

$$\text{tBMD} = (1 \quad \rho \quad S_g) \begin{pmatrix} \beta_1 \\ \beta_2 \\ \beta_3 \end{pmatrix} + (1 \quad 1) \begin{pmatrix} \delta_1 \\ \delta_2 \end{pmatrix} + \epsilon \quad (14)$$

Where δ_1 and δ_2 represent the intercept and the slope for each different individual respectively. To test the hypothesis of no interaction between the BV/TV and the group, i.e. the group has no significant influence on the tBMD versus BV/TV slope, the previous model was modified to add the interaction regressor.

$$\text{tBMD} = (1 \quad \rho \quad S_g \quad \rho S_g) \begin{pmatrix} \beta_1 \\ \beta_2 \\ \beta_3 \\ \beta_4 \end{pmatrix} + (1 \quad 1) \begin{pmatrix} \delta_1 \\ \delta_2 \end{pmatrix} + \epsilon \quad (15)$$

B. Extreme ROI Examples

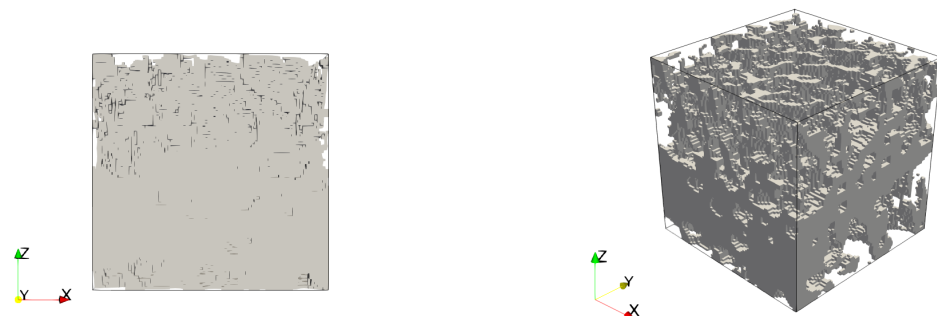


Figure 8: ROI with maximum BV/TV observed. BV/TV: 0.59; CV:0.19; DA:1.48. Left: front view; right: isometric view

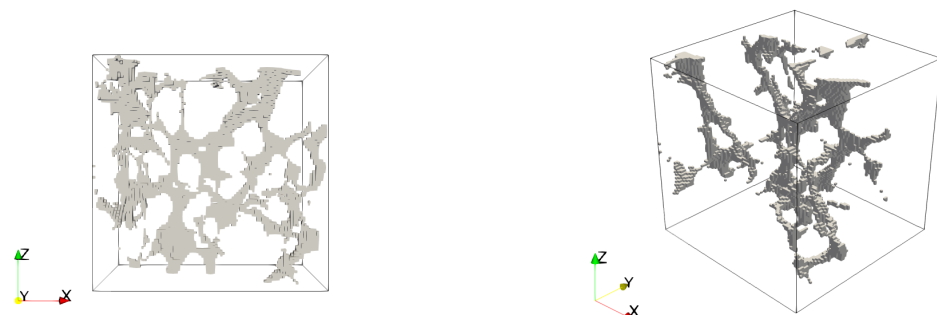


Figure 9: ROI with minimum BV/TV after filtering. BV/TV: 0.04; CV:0.19; DA:1.58. Left: front view; right: isometric view

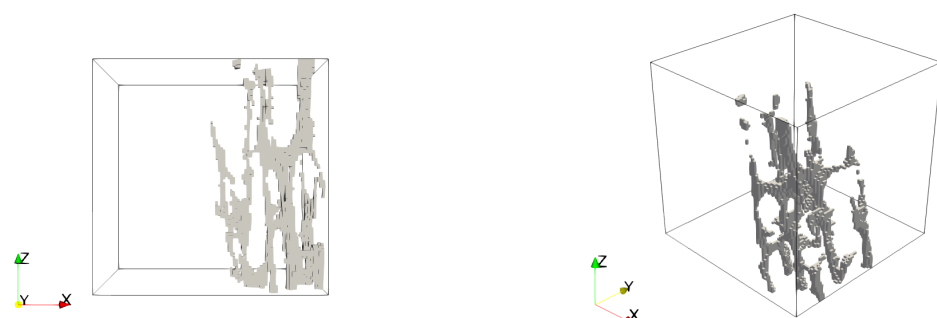


Figure 10: ROI with maximum CV observed. BV/TV: 0.02; CV:1.56; DA:2.25. Left: front view; right: isometric view

References

- [1] Agarwal, S., Rosete, F., Zhang, C., McMahon, D.J., Guo, X.E., Shane, E., Nishiyama, K.K., 2016. In vivo assessment of bone structure and estimated bone strength by first- and second-generation HR-pQCT. *Osteoporosis International* 27, 2955–2966. URL: <http://dx.doi.org/10.1007/s00198-016-3621-8>, doi:10.1007/s00198-016-3621-8.
- [2] Arias-Moreno, A.J., Hosseini, H.S., Bevers, M., Ito, K., Zysset, P., van Rietbergen, B., 2019. Validation of distal radius failure load predictions by homogenized- and micro-finite element analyses based on second-generation high-resolution peripheral quantitative CT images. *Osteoporosis International* 30, 1433–1443. doi:10.1007/s00198-019-04935-6.
- [3] Boutroy, S., Bouxsein, M.L., Munoz, F., Delmas, P.D., 2005. In vivo assessment of trabecular bone microarchitecture by high-resolution peripheral quantitative computed tomography. *Journal of Clinical Endocrinology and Metabolism* 90, 6508–6515. doi:10.1210/jc.2005-1258.
- [4] Boutroy, S., Van Rietbergen, B., Sornay-Rendu, E., Munoz, F., Bouxsein, M.L., Delmas, P.D., 2008. Finite element analysis based on in vivo HR-pQCT images of the distal radius is associated with wrist fracture in postmenopausal women. *Journal of Bone and Mineral Research* 23, 392–399. doi:10.1359/jbmr.071108.
- [5] Cowin, S.C., 1985. The relationship between the elasticity tensor and the fabric tensor. *Mechanics of Materials* 4, 137–147. URL: <http://www.sciencedirect.com/science/article/pii/0167663685900122>, doi:[https://doi.org/10.1016/0167-6636\(85\)90012-2](https://doi.org/10.1016/0167-6636(85)90012-2).
- [6] Daszkiewicz, K., Maquer, G., Zysset, P.K., 2017. The effective elastic properties of human trabecular bone may be approximated using micro-finite element analyses of embedded volume elements. *Biomechanics and Modeling in Mechanobiology* 16, 731–742. doi:10.1007/s10237-016-0849-3.
- [7] Folkestad, L., Hald, J.D., Hansen, S., Gram, J., Langdahl, B., Abrahamsen, B., Brixen, K., 2012. Bone geometry, density, and microarchitecture in the distal radius and tibia in adults with osteogenesis imperfecta type i assessed by high-resolution pQCT. *Journal of Bone and Mineral Research* 27, 1405–1412. doi:10.1002/jbmr.1592.
- [8] Fox, J., 2016. *Fox, Applied Regressions Analysis and Linear Models*. 3 ed.
- [9] Gross, T., Pahr, D.H., Zysset, P.K., 2013. Morphology elasticity relationships using decreasing fabric information of human trabecular bone from three major anatomical locations. *Biomechanics and Modeling in Mechanobiology* , 793–800doi:10.1007/s10237-012-0443-2.
- [10] Harrigan, T.P., Mann, R.W., 1985. Characterization of microstructural anisotropy in cancellous bone using a second rank tensor. *Journal of Materials Science* 19, 761–767.
- [11] Indermauer, M., Casari, D., Kochetkova, T., Peruzzi, C., Zimmermann, E., Rauch, F., Willie, B., Michler, J., Schwiedrzik, J., Zysset, P., 2021. Compressive Strength of Iliac Bone ECM Is Not Reduced in Osteogenesis Imperfecta and Increases With Mineralization. *Journal of Bone and Mineral Research* doi:10.1002/jbmr.4286.
- [12] Kocjan, R., Muschitz, C., Haschka, J., Hans, D., Nia, A., Geroldinger, A., Ardel, M., Wakolbinger, R., Resch, H., 2015. Bone structure assessed by HR-pQCT, TBS and DXL in adult patients with different types of osteogenesis imperfecta. *Osteoporosis International* 26, 2431–2440. doi:10.1007/s00198-015-3156-4.
- [13] Laird, N.M., Ware, J.H., 1982. Random-Effects Models for Longitudinal Data. *Biometrics* 38, 963–974.
- [14] Lim, J., Grafe, I., Alexander, S., Lee, B., 2017. Genetic causes and mechanisms of osteogenesis imperfecta. *Bone* 102, 40–49. URL: <https://www.sciencedirect.com/science/article/pii/S8756328217300492>, doi:<https://doi.org/10.1016/j.bone.2017.02.004>. rare Bone Diseases.
- [15] Lindahl, K., Åström, E., Rubin, C.J., Grigelioniene, G., Malmgren, B., Ljunggren, Ö., Kindmark, A., 2015. Genetic epidemiology, prevalence, and genotype-phenotype correlations in the Swedish population with osteogenesis imperfecta. *European Journal of Human Genetics* 23, 1042–1050. doi:10.1038/ejhg.2015.81.
- [16] Mandel, J., 1965. Generalisation de la theorie de plas-
- tice de w. t. koiter. *International Journal of Solids and Structures* 1, 273–295. URL: <https://www.sciencedirect.com/science/article/pii/002076836590034X>, doi:[https://doi.org/10.1016/0020-7683\(65\)90034-X](https://doi.org/10.1016/0020-7683(65)90034-X).
- [17] Moreno, R., Borga, M., Smedby, Ö., 2014. Techniques for computing fabric tensors: A review. *Mathematics and Visualization* , 271–292doi:10.1007/978-3-642-54301-2_12.
- [18] Mortier, G.R., Cohn, D.H., Cormier-Daire, V., Hall, C., Krakow, D., Mundlos, S., Nishimura, G., Robertson, S., Sangiorgi, L., Savarirayan, R., Sillence, D., Superti-Furga, A., Unger, S., Warman, M.L., 2019. Nosology and classification of genetic skeletal disorders: 2019 revision. *American Journal of Medical Genetics, Part A* 179, 2393–2419. doi:10.1002/ajmg.a.61366.
- [19] Pahr, D.H., Zysset, P.K., 2009. A comparison of enhanced continuum FE with micro FE models of human vertebral bodies. *Journal of Biomechanics* 42, 455–462. URL: <http://www.sciencedirect.com/science/article/pii/S0021929008006064>, doi:10.1016/j.jbiomech.2008.11.028.
- [20] Panyasantisuk, J., Pahr, D.H., Gross, T., Zysset, P.K., 2015. Comparison of Mixed and Kinematic Uniform Boundary Conditions in Homogenized Elasticity of Femoral Trabecular Bone Using Microfinite Element Analyses. *Journal of Biomechanical Engineering* 137, 1–7. doi:10.1115/1.4028968.
- [21] Pialat, J.B., Burghardt, A.J., Sode, M., Link, T.M., Majumdar, S., 2012. Visual grading of motion induced image degradation in high resolution peripheral computed tomography: Impact of image quality on measures of bone density and micro-architecture. *Bone* 50, 111–118. URL: <http://dx.doi.org/10.1016/j.bone.2011.10.003>, doi:10.1016/j.bone.2011.10.003.
- [22] Rolvien, T., Stürznickel, J., Schmidt, F.N., Butscheidt, S., Schmidt, T., Busse, B., Mundlos, S., Schinke, T., Kornak, U., Amling, M., Oheim, R., 2018. Comparison of Bone Microarchitecture Between Adult Osteogenesis Imperfecta and Early-Onset Osteoporosis. *Calciified Tissue International* 103, 512–521. URL: <http://dx.doi.org/10.1007/s00223-018-0447-8>, doi:10.1007/s00223-018-0447-8.
- [23] Schenk, D., Mathis, A., Lippuner, K., Zysset, P., 2020. In vivo repeatability of homogenized finite element analysis based on multiple HR-pQCT sections for assessment of distal radius and tibia strength. *Bone* 141, 115575. URL: <https://doi.org/10.1016/j.bone.2020.115575>, doi:10.1016/j.bone.2020.115575.
- [24] Scheres, L.J., van Dijk, F.S., Harsevoort, A.J., van Dijk, A.T., Domisse, A.M., Janus, G.J., Franken, A.A., 2018. Adults with osteogenesis imperfecta: Clinical characteristics of 151 patients with a focus on bisphosphonate use and bone density measurements. *Bone Reports* 8, 168–172. URL: <https://doi.org/10.1016/j.bonr.2018.04.009>, doi:10.1016/j.bonr.2018.04.009.
- [25] Tournis, S., Dede, A.D., 2018. Osteogenesis imperfecta A clinical update. *Metabolism: Clinical and Experimental* 80, 27–37. URL: <https://doi.org/10.1016/j.metabol.2017.06.001>, doi:10.1016/j.metabol.2017.06.001.
- [26] Varga, P., Dall'Ara, E., Pahr, D.H., Pretterklober, M., Zysset, P.K., 2011. Validation of an HR-pQCT-based homogenized finite element approach using mechanical testing of ultra-distal radius sections. *Biomechanics and Modeling in Mechanobiology* 10, 431–444. doi:10.1007/s10237-010-0245-3.
- [27] Whittier, D.E., Boyd, S.K., Burghardt, A.J., Paccou, J., Ghasem-Zadeh, A., Chapurlat, R., Engelke, K., Bouxsein, M.L., 2020. Guidelines for the assessment of bone density and microarchitecture in vivo using high-resolution peripheral quantitative computed tomography. *Osteoporosis International* 31, 1607–1627. doi:10.1007/s00198-020-05438-5.
- [28] Zysset, P.K., Curnier, A., 1995. An alternative model for anisotropic elasticity based on fabric tensors. *Mechanics of Materials* 21, 243–250. doi:10.1016/0167-6636(95)00018-6.
- [29] Zysset, P.K., Goulet, R.W., Hollister, S.J., 1998. A global relationship between trabecular bone morphology and homogenized elastic properties. *Journal of Biomechanical Engineering* 120, 640–646. doi:10.1115/1.2834756.